Single-Cell-Kinetics Approach to Compare Multidrug Resistance-Associated Membrane Transport in Subpopulations of Cells

ARTICLE *in* ANALYTICAL CHEMISTRY · AUGUST 2011

Impact Factor: 5.64 · DOI: 10.1021/ac201690t · Source: PubMed

2 AUTHORS, INCLUDING:

Sergey N Krylov
York University

167 PUBLICATIONS **3,624** CITATIONS

SEE PROFILE

analytical chemistry

LETTER

pubs.acs.org/ac

Single-Cell-Kinetics Approach to Compare Multidrug Resistance-Associated Membrane Transport in Subpopulations of Cells

Vasilij Koshkin and Sergey N. Krylov*

Department of Chemistry and Centre for Research on Biomolecular Interactions, York University, Toronto, Ontario M3J 1P3, Canada

Supporting Information

ABSTRACT: Multidrug resistance (MDR) driven by active efflux of drugs from the cells is one of the major obstacles in chemotherapies. Understanding the nature of MDR and designing more efficient chemotherapies requires the comparison of the efflux rate between different subpopulations of cells. Here we propose a single-cell-kinetics approach for such a comparison. In essence, the entire cell population is loaded with a suitable fluorescent substrate for MDR-associated membrane transporters. The kinetics of substrate efflux from individual cells is followed by time-lapse fluorescence microscopy and analyzed at the single-cell level. Microscopy is also used to assign cells to different subpopulations based on differences in morphology or level of staining by molecular probes. The kinetic parameters obtained for individual cells are then averaged for different cell subpopulations and the mean values of these parameters are finally compared between subpopulations. To test our single-cell-kinetics approach, we studied MDR-related efflux for two subpopulations of cultured breast cancer cells: cells in 2N and 4N phases of the cell cycle. The assignment of cells to 2N and 4N subpopulations was done by fluorescent DNA staining after the completion of efflux. By using the single-cell-kinetics approach, we were able to prove for the first time that the rates of MDR-related efflux differ in 2N and 4N phases of the cell cycle. We foresee that this approach will be an important tool in studies of MDR and in designing combination chemotherapies.

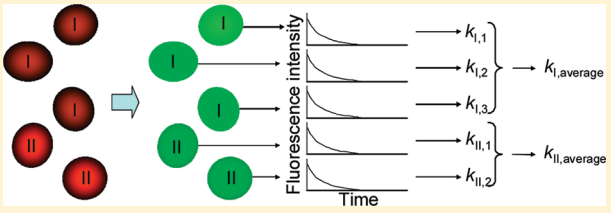

Multidrug resistance (MDR) due to active drug efflux from cells is arguably the major cause for failing chemotherapeutic treatments of cancer.[1] The MDR-associated drug efflux is driven by a superfamily of ATP-binding cassette (ABC) plasma membrane transporters.[2] Heterogeneous tissues may contain subpopulations of cells with different rates of efflux; the subpopulations with higher rates may survive chemotherapy and establish a chemotherapy-resistant tumor.[3] Understanding the nature of MDR and designing more efficient chemotherapies thus requires the comparison of the efflux rate between different subpopulations of cells. Such comparative studies have been hampered by the limitations in the technological approaches used for kinetic analyses of MDR-associated efflux. Up until now, efflux kinetics have only been studied using a population approach, in which a single kinetic trace is measured for the entire cell population and the kinetic parameters are obtained from this trace.[4] The population-based kinetic approach has, however, been shown to produce significant errors in the kinetic parameters.[5] To solve this problem and facilitate the comparison of efflux kinetics between subpopulations, we propose a single-cell-kinetics approach based, in its proof-of-principle realization, on time-lapse fluorescence microscopy (Figure 1). Conceptually, microscopy is first used to assign cells to specific subpopulations based on either their morphological properties or on levels of staining with specific molecular probes. The cells are then loaded with a fluorescent substrate suitable for the ABC transporters expressed in the studied cell type. The efflux of the substrate is initiated by replacing the substrate-containing media with a substrate-free media and is monitored using time-lapse fluorescence microscopy. Fluorescence intensity from single cells is measured as a function of time and kinetic traces of "fluorescence vs time" are plotted for individual cells. Kinetic parameters characterizing the rate of efflux are determined for individual cells. The kinetic parameters are averaged for cells of the same subpopulation and the mean parameter values and distributions are compared between the subpopulations. Note that the assignment of the cells to a subpopulation can be performed after measuring the efflux kinetics, as was done in this work.

To test the single-cell-kinetics approach, we compared MDR-associated membrane transport in the 2N and 4N subpopulations of breast cancer cells (MCF 7 cell line). A cell normally has two sets of chromosomes (2N) but when it progresses through the cell cycle it replicates its DNA and before dividing into two daughter cells it has 4 sets of chromosomes (4N). It has previously been reported that 4N cells have a greater level of ABC transporter expression than the 2N cells,[6] but the MDR-associated membrane transport rates have never been measured for 2N and 4N cell subpopulations. Measuring such rates was our goal.

Received: June 30, 2011
Accepted: July 19, 2011
Published: July 19, 2011

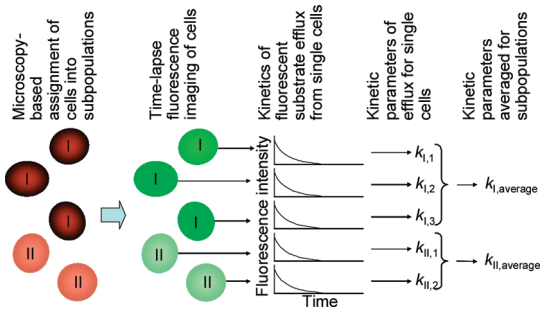

Figure 1. Schematic illustration of single-cell-kinetics approach for comparing MDR-associated membrane transport in subpopulations of cells. See text for details.

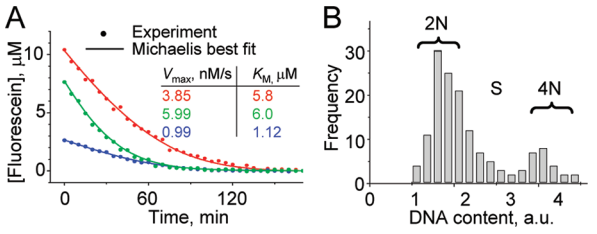

Figure 2. Results of the combined analysis of fluorescein efflux (A) and cell-cycle position determination (B). Fluorescein efflux is shown for 3 representative cells out of a total of 539 cells analyzed for kinetics. The DNA-content histogram is shown for cells (146) on a single plate.

The first task was to choose a suitable fluorescent substrate for monitoring the MDR-associated efflux. MCF-7 cells and other breast cancer cells have been reported to have ABC transporters of the multidrug-resistance related protein (MRP) family.[7] MRP transporters can pump out fluorescein and this transport can be inhibited by glyburide.[8] On the other hand, these transporters do not pump out rhodamine and mithoxantrone in an inhibitor-dependent fashion. We tested three different fluorescent substrate/inhibitor pairs, which are specific for three families of ABC transporters: fluorescein/glyburide, rhodamine 123/cyclosporine, and mithoxantrone/cyclosporine A.[9] A flow-cytometry study showed that only fluorescein was accumulated by cells in an inhibitor-dependent fashion (Figure S1 in the Supporting Information). We thus confirmed that our cell line had a MRP family of transporters[10] and that fluorescein was the right substrate for these cells.

The next task was to adapt our general approach for the individual cell, depicted in Figure 1, toward the comparative analysis of efflux kinetics in 2N and 4N cell subpopulations. 2N and 4N cells were distinguished by fluorescently staining genomic DNA with propidium iodide (PI), a DNA-intercalating dye (PI fluorescence of 4N cells is approximately 2 times brighter than that of 2N cells). DNA staining with PI required membrane permeabilization which would make the efflux experiments impossible afterward. Therefore, staining of cells with PI and assignment of cells to 2N and 4N subpopulations were performed after measuring the efflux kinetics. Cells with an intermediate amount of DNA (the cells in the S phase of the cell cycle) were disregarded. In addition, we tested the cells for apoptosis and apoptotic cells were also not taken into consideration. Fluorescein efflux measurements and the following cell assignment to 2N and 4N subpopulations were performed with the cell plate situated on the microscope stage. The manipulations were carried out with care to ensure that cell positions did not change and that single cells can be tracked throughout the entire experiment.

Below we describe the result of our experiments that combined measurements of efflux kinetics with determination of cell-cycle position. Cell images were recorded in a time-lapse mode at the wavelength of fluorescein fluorescence (520 nm) at an interval of 5 min during a 1.5−2.5 h period (Figure S2A in the Supporting Information). The cells were then stained with PI and a cell image was recorded at the fluorescence emission wavelength of PI (620 nm) (Figure S2B in the Supporting Information). The images were then processed, and fluorescence intensities originating from the intracellular volume of 757 individual cells grown on 5 plates were quantified. The intensities of fluorescein fluorescence were determined for every time point, and kinetic traces of fluorescein efflux were constructed for individual cells. Figure 2A shows representative traces for several individual cells with a visible difference in the efflux rates. The intensity of PI fluorescence was then determined for the same 757 cells. The cell cycle histograms had a typical bimodal shape with the majority of cells being in the 2N phase and a smaller number in the 4N phase of the cell cycle (see example in Figure 2B). After this we could analyze the kinetics of fluorescein efflux for 2N and 4N cells. A smaller number of cells were in the intermediate position, corresponding to the S phase of the cell cycle. These cells were not analyzed due to their relatively small abundance and difficulties in the unambiguous assignment to the S phase.[11]

The analysis of kinetic traces for individual cells revealed that fluorescein efflux followed Michaelis−Menten kinetics typical for enzymatic reactions. This result was not surprising. Membrane transporters can function in a way similar to enzymes by converting a substrate (intracellular fluorescein) into a product (extracellular fluorescein) through the formation of an intermediate transporter−substrate complex. In particular, Michaelis−Menten behavior of ABC transporters was previously observed in cell population experiments.[12] The efflux kinetics of single cells could thus be characterized by two Michaelis−Menten parameters, the maximum enzyme velocity, V_{max}, and the Michaelis−Menten constant, K_M. These parameters were determined for all 438 2N cells and 101 4N cells. Representative results for cells on a single plate are shown in Figure 3 as frequency histograms. The 4N cells had greater values of both V_{max} and the V_{max} to K_M ratio (V_{max}/K_M). These results together suggest that 4N cells have a greater activity (V_{max}) and efficiency (V_{max}/K_M) of MDR-associated fluorescein efflux than 2N cells. Both improved catalytic properties and increased expression of MDR transporters could contribute to the observed elevated rate of efflux in 4N cells. The correlation between MDR activity and cell cycle position has not been previously reported likely due to limitations in the population approach used for such studies.

To test whether or not the correlation between the MDR activity and the cell cycle position could be revealed with a population-kinetics approach, we applied the population-kinetics approach and processed the same data set of efflux kinetics. In essence, the fluorescent signal was averaged for every cell subpopulation (2N and 4N) for every time point and average kinetic traces for 2N and 4N cells were built. The values of V_{max} and V_{max}/K_M were calculated for these two kinetic traces and compared with the V_{max} and V_{max}/K_M values obtained with the single-cell-kinetics approach (Figure 4). The population-kinetics approach also shows a greater rate of fluorescein efflux from 4N

dx.doi.org/10.1021/ac201690t |Anal. Chem. 2011, 83, 6132–6134

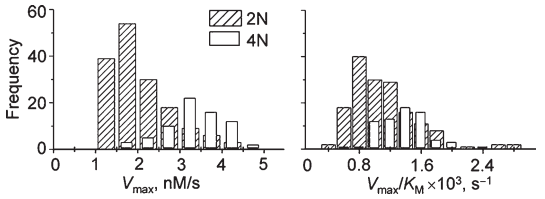

Figure 3. Distributions of V_{max} and V_{max}/K_M for cells in 2N and 4N subpopulations on a single plate (total of 159 2N cells and 70 4N cells).

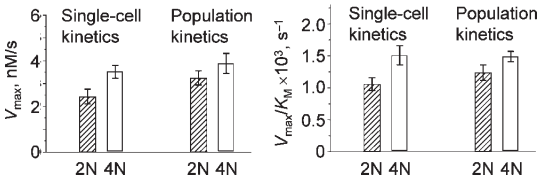

Figure 4. Kinetic parameters of MDR transport in 2N and 4N subpopulations of cells obtained from the single-cell-kinetics and population-kinetics approaches. In both cases, 438 2N calls and 101 4N cells were analyzed.

cells but the difference was below the statistically significant level. These results prove that the single-cell-kinetics approach is more sensitive for revealing the difference in MDR-associated transporter activity compared to the population-kinetics approach.

To conclude, we introduced a single-cell-kinetics approach to compare MDR-associated membrane transport in cell subpopulations. By using this approach, we were able to undoubtedly demonstrate that the rate of MDR-associated transport in cancer cells (MCF-7 breast cancer cell line) changes with cell progression through the cell cycle. This finding is important as cell-cycle arresting agents are often used in combination chemotherapies and understanding MDR dependence on the cell cycle can help in choosing the most suitable cell-cycle arresting and/or cytotoxic agent. Therefore, our single-cell approach will be an important tool in studies of MDR and in designing combination chemotherapies. Moreover, our finding suggests that the single-cell approach should be given preference over population-based approaches when studying kinetics. In our view, cell handling in microfluidic devices, which proved to be very reliable,[13] can significantly improve single-cell-kinetics measurements.

■ ASSOCIATED CONTENT

Ⓢ Supporting Information. Supporting materials and methods and supporting figures. This material is available free of charge via the Internet at http://pubs.acs.org.

■ AUTHOR INFORMATION

Corresponding Author

*E-mail: skrylov@yorku.ca.

■ ACKNOWLEDGMENT

The work was funded by the Natural Sciences and Engineering Research Council of Canada.

■ REFERENCES

(1) Shukla, S.; Ohnuma, S.; Ambudkar, S. V. *Curr. Drug Targets* **2011**, *12*, 621–630.

(2) (a) Gottesman, M. M. *Annu. Rev. Med.* **2002**, *53*, 615–627.(b) Bernaudin, J. F.; Fajac, A.; Fleury-Feith, J.; Kerrou, K.; Lacave, R. In *ABC Transporters and Multidrug Resistance*; Boumendjel, A., Ed.; John Wiley & Sons, Inc.: Hoboken, NJ, 2009; pp 143−176.

(3) (a) Katayama, R.; Koike, S.; Sato, S.; Sugimoto, Y.; Tsuruo, T.; Fujita, N. *Cancer Sci.* **2009**, *100*, 2060–2068. (b) Moitra, K.; Lou, H.; Dean, M. *Clin. Pharmacol. Ther.* **2011**, *89*, 491–502.

(4) (a) Saengkhae, C.; Loetchutinat, C.; Garnier-Suillerot, A. *Biophys. J.* **2003**, *85*, 2006–2014. (b) Saengkhae, C.; Loetchutinat, C.; Garnier-Suillerot, A. *Biochem. Pharmacol.* **2003**, *65*, 969–977. (c) Zhou, C.; Shen, P.; Cheng, Y. *Biochim. Biophys. Acta* **2007**, *1770*, 1011–1020.

(5) Wong, W. W.; Tsai, T. Y.; Liao, J. C. *Mol. Syst. Biol.* **2007**, *3*, 130.

(6) Ramachandran, C.; Mead, D.; Wellham, L. L.; Sauerteig, A.; Krishan, A. *Biochem. Pharmacol.* **1995**, *49*, 545–552.

(7) Kars, M. D.; Iseri, O. D.; Gunduz, U.; Ural, A. U.; Arpaci, F.; Molnar, J. *Anticancer Res.* **2006**, *26*, 4559–4568.

(8) He, S. M.; Li, R.; Kanwar, J. R.; Zhou, S. F. *Curr. Med. Chem.* **2011**, *18*, 439–481.

(9) Eckford, P. D.; Sharom, F. J. *Chem. Rev.* **2009**, *109*, 2989–3011.

(10) (a) Keppler, D. *Handb. Exp. Pharmacol.* **2011**, *201*, 299–323. (b) Deeley, R. G.; Cole, S. P. *FEBS Lett.* **2006**, *580*, 1103–1111.

(11) (a) Bauer, T. W.; Tubbs, R. R.; Edinger, M. G.; Suit, P. F.; Gephardt, G. N.; Levin, H. S. *Am. J. Clin. Pathol.* **1990**, *93*, 322–326. (b) Claud, R. D., 3rd; Weinstein, R. S.; Howeedy, A.; Straus, A. K.; Coon, J. S. *Mod. Pathol.* **1989**, *2*, 463–467.

(12) (a) Stein, W. D. *Physiol. Rev.* **1997**, *77*, 545–590. (b) Slot, A. J.; Wise, D. D.; Deeley, R. G.; Monks, T. J.; Cole, S. P. *Drug Metab. Dispos.* **2008**, *36*, 552–560.

(13) Li, X.; Chen, Y.; Li, P. C. *Lab Chip* **2011**, *11*, 1378–1384.

SUPPORTING INFORMATION

Single-Cell-Kinetics Approach to Compare Multidrug Resistance-Associated Membrane Transport in Subpopulations of Cells

Vasilij Koshkin and Sergey N. Krylov

Department of Chemistry and Centre for Research on Biomolecular Interactions, York University, Toronto, Ontario, M3J 1P3, Canada

Table of Contents

1. Supporting Materials and Methods

1.1. Chemicals and materials. The human breast cancer cell line MCF-7 was obtained from the American Type Culture Collection (ATCC, Manassas, VA; ATCC # HTB-22). The cells were maintained in the supplier-recommended media and supplements at 37°C in a humidified 5% CO_2 environment and used within culturing period of shorter than 6 months. Fluorescent dyes rhodamine 123, fluorescein, mithoxantrone, and propidium iodide (PI) were purchased from Sigma-Aldrich (St. Louis, MO). All other reagents were from Sigma-Aldrich, Fluka AG (Buchs, Switzerland), and BDH Chemicals Ltd. (Poole, England).

1.2. Measurement of accumulation of fluorescent MDR probes in cell populations by flow cytometry. Cellular content of fluorescent MDR probes was measured by flow cytometry using a BD FACSCanto II flow cytometer (BD Biosciences, Franklin Lakes, NJ). Cell suspensions at approximately 10^6 cells/mL were loaded with a probe (1-5 μM, 30-45 min, 37ºC) in KRB buffer containing 140 mM NaCl, 3 mM KCl, 10 mM Na_2HPO_4, 2 mM KH_2PO_4, 2 mM $CaCl_2$, 1 mM $MgCl_2$, and 10 mM glucose. After being loaded with the probe, cells were gently spun down, washed, re-suspended in fresh medium (containing 5 μM PI) and examined by flow cytometry for probe accumulation using a standard argon-ion laser for excitation at 488-nm with a 530/30 nm band pass filter for the emission of rhodamine 123, calcein, and fluorescein and a 585/42 band pass filter for the emission of PI. To evaluate the accumulation of mitoxantrone, samples were excited with a 635-nm red diode laser, and a 680/32 band pass filter was used to measure its emission.

1.3. Measurement of accumulation and efflux of fluorescent MDR probe in single cells by fluorescent imaging. Cell monolayers of approximately 50% confluence were loaded with 5 μM fluorescein for 30 min at 37ºC in the presence of 10 μM glyburide, washed free of extracellular probe and MDR inhibitor, and placed in KRB buffer. The kinetics of fluorescein efflux were monitored using a laser scanning confocal fluorescence microscope (Fluoview FV300, Olympus, Japan), with argon-ion laser excitation at 488 nm and Omega filter set XF75 (Omega Optical, Inc. Brattleboro, VT) following an approach described elsewhere.[1]

1.4. Determination of cell viability and cell cycle phase. After completing the kinetic measurements, cells were loaded with PI (10 μM, 10 min) to discriminate apoptotic cells from live cells. Afterwards, treatment with the plasma membrane-specific surfactant, saponin (80 μg/mL) and RNAase A (0.02 mg/mL) provided PI access to all nuclei and allowed for the removal of cellular RNA. The fluorescent signal from PI-stained cells was imaged with a green

Kr laser and Omega filter set XF35 (Omega Optical, Inc. Brattleboro, VT), quantified, and used for the determination of (the) specific cell cycle phase. Cells intermediary to the 2N and 4N states (S fraction) were excluded from consideration which is customary in imaging investigations of cell cycle due to difficulties in their identification and innumerous populations.[2,3] 2N and 4N cells were analytically discriminated from the intermediate fraction using the half-maximum height criterion.[4]

1.5. Kinetic fitting and simulation methods. Experimental progress curves of fluorescein efflux were fit, and the transport kinetics were simulated using the integrated Michaelis-Menten equation for a single-substrate irreversible reaction:

$$V_{max}t = ([S]_0 - [S]) + K_M \ln([S]_0 / ([S]_0 - [S])$$

where $[S]_0$ and $[S]$ are the initial and current substrate concentrations, respectively.[5,6] Calculations were performed using KaleidaGraph (Synergy Software, Reading, PA) and Origin (Microcal Software, Northampton, MA) software.

2. Supporting References

1) Krylov, S.N.; Zhang, Z.; Chan, N.W.; Arriaga, E.; Palcic, M.M.; Dovichi, N.J. Correlating cell cycle with metabolism in single cells: combination of image and metabolic cytometry. *Cytometry* **1999**, *37*, 14-20.

2) Bauer, T.W.; Tubbs, R.R.; Edinger, M.G.; Suit, P.F.; Gephardt, G.N.; Levin, H.S. A prospective comparison of DNA quantitation by image and flow cytometry. *Am. J. Clin. Pathol.* **1990**, *93*, 322-326.

3) Claud RD, 3rd, Weinstein RS, Howeedy A, Straus AK, Coon JS. Comparison of image analysis of imprints with flow cytometry for DNA analysis of solid tumors. *Mod. Pathol.* **1989**, 2, 463-467.

4) Sinclair, W.K.; Ross, D.W. Modes of growth in mammalian cells. *Biophys. J.* **1969**, *9*, 1056-1070.

5) Duggleby, R.G. Analysis of enzyme progress curves by nonlinear regression. *Methods Enzymol.* **1995**, 249, 61-90.

6) Stein, R.L.; Barbosa, M.D.; Bruckner, R. Kinetic and mechanistic studies of signal peptidase I from Escherichia coli. *Biochemistry* **2000**, *39*, 7973-7983.

3. Supporting Figures

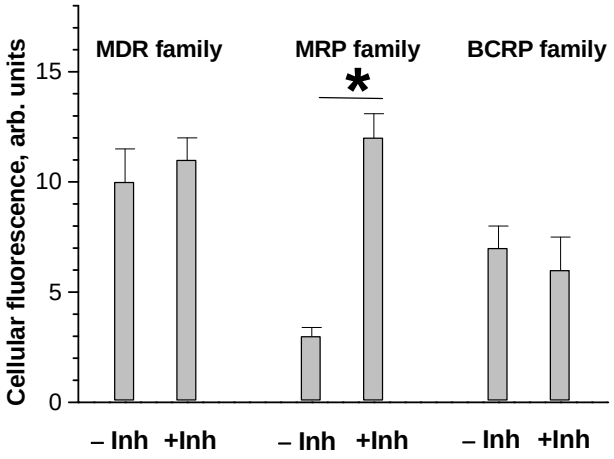

Figure S1. Selection of appropriate fluorescent substrate for studying MDR kinetics in MCF-7 cells. Cells were loaded with substrates specific for different families of ABC transporters in the absence and presence of appropriate transport inhibitors: (i) rhodamine 123 with or without cyclosporine A (-/+ inh) for the MDR family of transporters, (ii) fluorescein with or without glyburide for the MRP family of transporters, (iii) mithoxantrone with or without cyclosporine A for BCRP family of transporters.

A

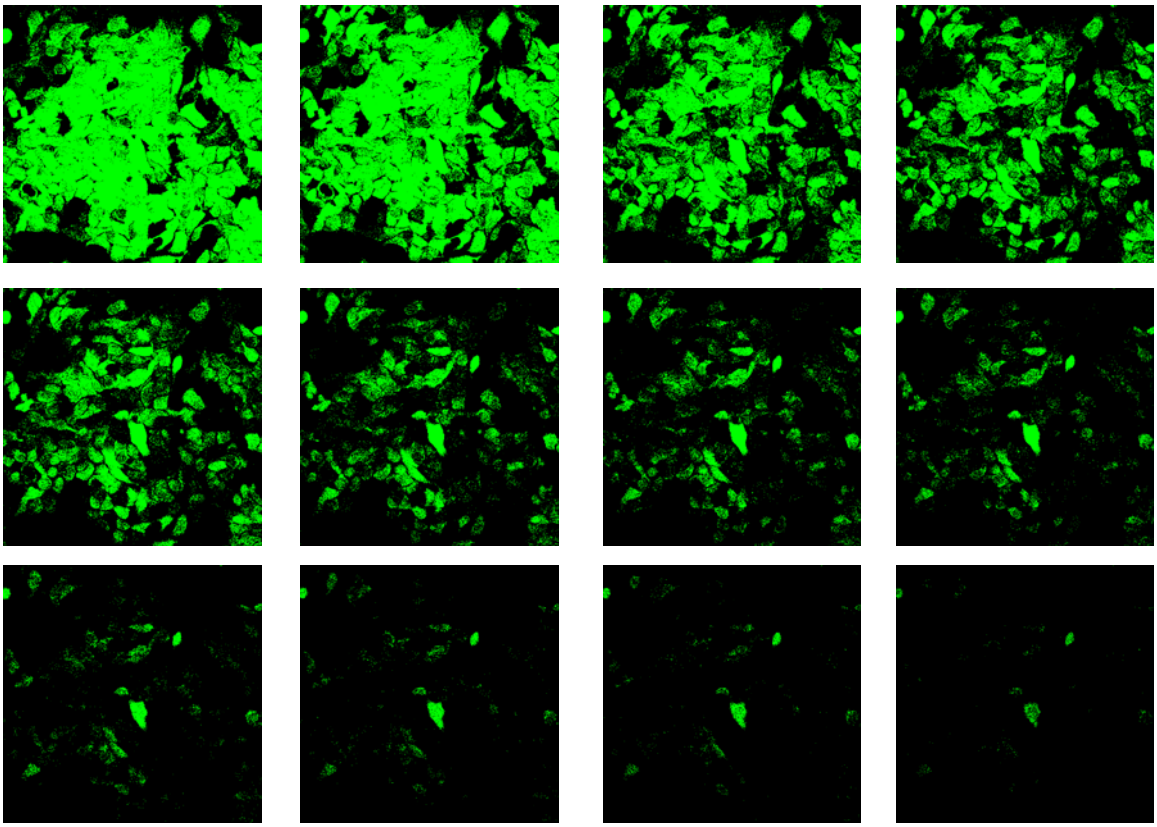

B

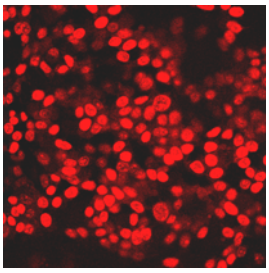

Figure S2. Representative images of fluorescein-loaded (A) and PI-stained (B) cells. Images in Panel **A** were taken with a 10-min interval, image in panel **B** was taken for the same cells after their final treatment with PI.